Environmental Challenges 4 (2021) 100122

Contents lists available at ScienceDirect

Environmental Challenges

journal homepage: www.elsevier.com/locate/envc

Spatial distribution of heatwave vulnerability in a coastal city of Bangladesh

Debasish Roy Raja [a], Md Shah Naim Hredoy [a,c], Md. Kamrul Islam [a], K.M. Ashraful Islam [a], Mohammed Sarfaraz Gani Adnan [a,b,*]

[a] Department of Urban and Regional Planning, Chittagong University of Engineering and Technology, Chattogram 4349, Bangladesh
[b] Environmental Change Institute, School of Geography and the Environment, University of Oxford, OX1 3QY, United Kingdom
[c] Department of Earth Sciences, University of Memphis, Memphis, TN 38152, United States

ARTICLE INFO

Keywords:
Heatwave hazard
Exposure
Sensitivity
Adaptive capacity
Factor Analysis
Spatial Statistics Analysis

ABSTRACT

While extreme heat events received wider attention in recent years, understanding heatwave vulnerability is still a challenging task that requires a clear understanding of a range of location-dependent climatic, socio-economic, physiological, and environmental parameters. This study investigates the spatial distribution of heatwave vulnerability in Chattogram City Corporation (CCC) — the commercial capital of Bangladesh. A heatwave vulnerability index (HVI) was developed, including various parameters related to three latent variables — exposure, sensitivity, and adaptive capacity — derived using remote sensing and socio-economic data. Factor analysis was performed to assess all parameters related to HVI. Besides, spatial autocorrelation, cluster and outlier analyses, and hot spot analysis were carried out to investigate the spatial distribution of HVI. This study shows a spatial distribution of HVI in CCC, which is spatially associated with various individual parameters. A total of seven wards (smallest administrative zone of CCC) were found to be very highly vulnerable to the heatwave. This study further reveals that heatwave vulnerability is randomly distributed throughout the city, although the high land surface temperature is concentrated in the existing built-up areas. It also identified three major hot spots of heatwave vulnerability in CCC. The methodology and findings of this study will be of interest to the policymakers and city planners to prepare mitigation plans, policies, and strategies to mitigate this hazard.

Introduction

Weather extremes such as extreme heat events have become more frequent and severe in recent years in the face of climate change leading to global warming (Aubrecht and Özceylan, 2013; Azhar et al., 2017; Ho et al., 2015). Thus, heat-related morbidity (e.g., diarrhea, respiratory diseases, heat exhaustion, and heat stroke) and mortality have increased globally, particularly in tropical, subtropical, and temperate climate zones (Basagaña et al., 2011; Ho et al., 2015; Rinner et al., 2010). Elder people (aged over 60 years) and children are more vulnerable to these extreme events (Aubrecht and Özceylan, 2013). Countries both in developed and developing worlds experienced detrimental effects of extreme heat events in the recent past. For instance, recent studies reported a significant number of causalities due to illness caused by extreme heat waves in various countries across the world, such as Australia (Zhang et al., 2017), Bangladesh (Arrighi et al., 2017), China (Chen et al., 2017), India (Azhar et al., 2017), Russia (Dole et al., 2011), UK (Wolf and McGregor, 2013), and the USA (Ogbomo et al., 2017).

Studies related to heatwave vulnerability and risk have received wider attention recently (Aubrecht and Özceylan, 2013; Azhar et al., 2017; Ho et al., 2015; Kim et al., 2017; Liu et al., 2020). Conceptually, heatwave vulnerability is the product of three latent factors: exposure, sensitivity, and adaptive capacity (Mac and McCauley, 2017). Exposure refers to the presence of people, livelihoods, environmental services and resources, infrastructure, or economic, social, or cultural assets proximity to extreme events, causing potential future harm, loss, or damage. Sensitivity or fragility is the physical predisposition of human beings, infrastructure, and the environment to be affected by hazardous events due to lack of resistance (Field et al., 2012; Zuhra et al., 2019). Adaptive capacity is "the ability of an individual, family, community, or other social groups to adjust to changes in the environment guaranteeing survival and sustainability" (Lavell, 1999). Most of the recent studies related to heat vulnerability emphasized exposure and sensitivity parameters while developing a heat vulnerability index (Aubrecht and Özceylan, 2013; Azhar et al., 2017; Christenson et al., 2017; Harlan et al., 2013; Inostroza et al., 2016; Johnson et al., 2012;

* Corresponding author at: Department of Urban and Regional Planning, Chittagong University of Engineering and Technology, Chattogram 4349, Bangladesh.
E-mail address: sarfarazadnan@cuet.ac.bd (M.S.G. Adnan).

https://doi.org/10.1016/j.envc.2021.100122
Received 14 March 2021; Received in revised form 17 April 2021; Accepted 18 April 2021
2667-0100/© 2021 The Author(s). Published by Elsevier B.V. This is an open access article under the CC BY-NC-ND license (http://creativecommons.org/licenses/by-nc-nd/4.0/)

Macnee and Tokai, 2016; Mushore et al., 2018; Nayak et al., 2018; Wolf and McGregor, 2013). Only a few studies considered all three aspects of vulnerability. For instance, Inostroza et al. (2016) developed a heat vulnerability index applying a Geographic Information System (GIS)-based approach, where exposure, sensitivity, and adaptive capacity were derived from remote sensing and various socioeconomic data. Zuhra et al. (2019) applied a similar approach to estimate heatwave vulnerability. Mac and McCauley (2017) proposed a conceptual framework for evaluating heatwave vulnerability integrating three factors: exposure, sensitivity and adaptive capacity, and the heat stress response.

Evaluating the spatial distribution of heatwave vulnerability is a complex process that requires a clear understanding of a range of location-dependent climatic, socio-economic, physiological, and environmental parameters (Aubrecht and Özceylan, 2013; Azhar et al., 2017; Zuhra et al., 2019). The development of GIS and remote sensing technology in the last few decades has enabled researchers to assess the extent of heat stress vulnerability efficiently (Inostroza et al., 2016; Mushore et al., 2018). Remote sensing data offers several advantages that enable accurate observation of land surface temperature, develop medium to high-resolution maps, and provide access to long time-series data (Mushore et al., 2018).

Bangladesh is one of the most climate-sensitive countries globally, where the frequency and severity of heatwave are predicted to increase in the future (Nissan et al., 2017). A significant number of deaths in Bangladesh are associated with increased heatwave severity, as mortality tends to increase by 31.3% with a 1 ˚C increase in the universal thermal climate index. Older people aged over 65 are the most vulnerable to heat-related diseases (Burkart et al., 2014). Coastal city Chattogram is the second-largest city and the commercial capital of this country (Adnan et al., 2019). Like other major cities (e.g., Dhaka) of Bangladesh (Dewan and Yamaguchi, 2009), unplanned and uncontrolled urbanization, urban sprawl, and anthropogenic activities are causing a change in the local and micro-level climate of Chattogram city (Ara et al., 2016; Gazi et al., 2020). A recent study reveals that surface urban heat island intensity (SUHII) (day and night) in five major cities of Bangladesh has increased substantially during the last 20 years, where Chattogram city has experienced the highest increase in SUHII at night by 1.9 °C (Dewan et al., 2021). The existing thermal studies based on remote sensing techniques in Bangladesh are predominantly concentrated on investigating the drivers of increasing urban land surface temperature (Ahmed et al., 2013; Ara et al., 2016; Dewan and Corner, 2012; Gazi et al., 2020; Roy et al., 2020). In other regions, previous heatwave vulnerability related studies focused on the context of the semiarid Mediterranean climatic region (Inostroza et al., 2016), tropical region (Azhar et al., 2017; Mushore et al., 2018; Zhang et al., 2018; Zuhra et al., 2019), temperate zone (Kim et al., 2017), and the global north (Christenson et al., 2017; Johnson et al., 2012). However, understanding the environmental and anthropogenic impacts of extreme heatwave hazards in the context of a coastal megacity is still in its infancy. Besides, access to required data has always been a significant challenge in estimating heatwave vulnerability at a regional, city, or local scale (Inostroza et al., 2016). To address these gaps in the existing literature, this study aimed to investigate the spatial pattern of the heatwave vulnerability in Chattogram city by developing a heat vulnerability index (HVI), considering exposure, sensitivity, and adaptive capacity aspects of vulnerability.

Materials and methods

Study area

Chattogram City Corporation (CCC) area, located in the southeastern part of Bangladesh, was selected as the study area. The area lies between latitude 22°23′45″ and 22°13′42″ North, and longitude 91°45′26″ and 91°53′29″ East, bounded by the Karnafuli River to the southeast and the Bay of Bengal to the west (Fig. 1). This coastal city has a total area of 161 km^2 and comprises 41 wards (smallest administrative area) (BBS, 2011). Like other areas in Bangladesh, a tropical monsoon climate prevails in this city (Gazi et al., 2020). The city is regarded as the second most populated city in Bangladesh, where its second-largest industrial zone is located (Hoque and Clarke, 2013). The city is characterized by rapid urbanization and industrial development, which reportedly resulted in a loss of 26% forest area between 1991 and 2015, while built-up area increases to about 48% in that period (Ara et al., 2016). Due to the unplanned development in this city, the proportion of existing water bodies (e.g., Chaktai and Rajakhali) canal have reduced significantly in the last two to three decades (Hassan and Nazem, 2016).

Chattogram city has been experiencing harsh climatic conditions in recent years. For instance, this city's annual mean temperature has increased by 1.1 °C over the last two decades (BMD, 2019). Urban heat island effects were observed in urban centers and densely populated parts of the city. Unplanned urbanization, population growth, increase in the proportion of built-up areas, inadequate vegetation cover, and a lack of water body are reportedly associated with the increased surface temperature (Ara et al., 2016; Gazi et al., 2020; Roy et al., 2020). The increasing surface temperature increased heat-related illnesses such as heat stroke and skin cancer (Ara et al., 2016). An understanding of heatwave vulnerability is the prerequisite for developing a heat early warning system which is essential for formulating policies to reduce an abrupt increase in heat-related hazard (Nissan et al., 2017). Hence, this study aimed to develop an HVI for the CCC area.

Heatwave vulnerability index

In this study, the heatwave vulnerability index (HVI) was estimated as a function of exposure (*E*), sensitivity (*S*), and adaptive capacity (*A*) (Eq. (1)) (Inostroza et al., 2016). Exposure and sensitivity are the triggering factors of the HVI, while adaptive capacity reduces the vulnerability.

$$HVI = E + S - A \tag{1}$$

Based on an extensive review of the existing literature, several observed variables were identified to measure the three latent variables: exposure, sensitivity, and adaptive capacity (Table 1). Observed variables are those that can be readily measured from the field (Borsboom et al., 2003). Most of the variables were expressed in relative terms, i.e., per unit of surface (no/sq.km) to avoid the spatial bias induced by excessively large or very small administrative boundaries. The spatial distribution of different observed variables is given in Fig. S1 of the supplementary document.

Exposure

In this study, exposure was represented by LST and population density. Although LST is an indicator of heat hazard (Mac and McCauley, 2017), several recent studies argued that LST also indicates the intensity of heat exposure (Inostroza et al., 2016; Zuhra et al., 2019). LST is regarded as the most influential variable indicating heatwave vulnerability, as increased LST induces the frequency of heat-related diseases such as cardiovascular diseases, diarrhea, and respiratory diseases. Excessive heat also decreases the capability of humans to withstand the situation. Evidence from various studies indicated an increase in LST might increase heatwave vulnerability (Aubrecht and Özceylan, 2013; McGeehin and Mirabelli, 2001; Reid et al., 2009). The population density was considered another observed variable of exposure, as areas with high population density are the most assailable to heat (Tomlinson et al., 2011).

Sensitivity

Ten variables were identified to quantify the degree of sensitivity to the heatwave (Table 1). Older people are susceptible to heatwave due to their age and underlying medical problems like cardiovascular diseases (Aldrich and Benson, 2008; Aubrecht and Özceylan, 2013; Harlan et al.,

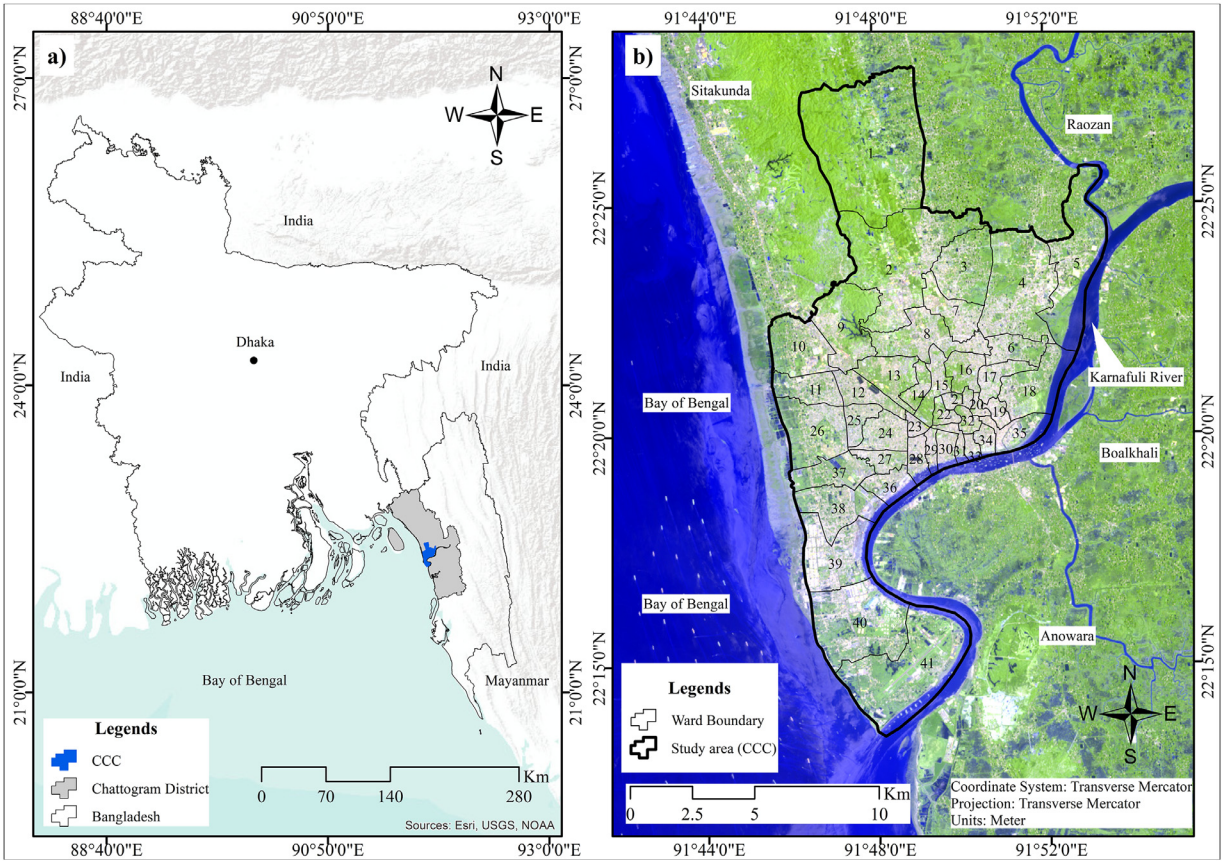

Fig. 1. Location map of the study area.

2006; McGeehin and Mirabelli, 2001; Semenza et al., 1996). Very young people, such as children aged below nine years, are also vulnerable to extreme heat events due to their susceptibility to different vector-borne diseases (Haines et al., 2006; Nakai et al., 1999; Wilhelmi and Hayden, 2010). Various studies demonstrated that illiterate people are sensitive to heat events, as they are not aware of these events' potential danger. Therefore, deaths caused by heat-related diseases are high among illiterate people (Cutter et al., 2003; Harlan et al., 2006; Medina-Ramón et al., 2006; O'Neill et al., 2003; Uejio et al., 2011).

The built-up area can also be associated with heath wave vulnerability, as these areas retain the heat from the sun longer than the surrounding environment, which contributes to the increase in overall temperature in a city. These areas potentially release more anthropogenic heat due to higher population density (Hoque and Clarke, 2013; Mushore et al., 2018; Nayak et al., 2018). Various socioeconomic condition of people is also reportedly associated with extreme heat events. For instance, a lack of access to information on heatwave vulnerability and utility facilities (e.g., electric fan, air condition, air cooler) of people living below the poverty line (population below $1.90 purchasing power parity/day according to the Asian Development Bank) make these group sensitive to heatwave vulnerability (McMichael et al., 2008; Patz et al., 2005; Poumadere et al., 2005). In the study area, the number of people living below the poverty line was between zero and 9200 persons/km^2. Access to the water supply is an essential indicator of heat sensitivity, as water is widely used for individual cooling purposes (Inostroza et al., 2016). In respect to people's demographic characteristics, the female population, particularly those who are pregnant, are comparatively more vulnerable to heat than men (Johnson et al., 2012). People's unemployment status is associated with poverty, making them susceptible to heatwave events (Buscail et al., 2012; Méndez-Lázaro et al., 2018; Mushore et al., 2018). Occupations that involve physical activity (e.g., agricultural activity, industrial works) are associated with heath vulnerability due to higher exposure to heat (Cutter et al., 2003). Disable people are also vulnerable as they are less capable of coping with any adverse condition resulting from extreme heat events (Inostroza et al., 2016).

Adaptive capacity

Four variables were identified to measure adaptive capacity: access to electricity, vegetation, road, and waterbody. Access to electricity can reduce heatwave vulnerability because people can use electrical devices such as a fan, AC, air cooler to reduce heat intensity (Kovats and Hajat, 2008). Vegetation cover is also an indicator of adaptive capacity. A higher proportion of vegetation cover could reduce the city's temperature and, thus, heatwave vulnerability (Hajat et al., 2007; Kinney et al., 2008). The indicator road is associated with traffic congestion. Adequate road infrastructure in a city would minimize vehicle congestion, therefore, less anthropogenic heat generation (Inostroza et al., 2016). The presence of water bodies can also reduce heat intensity, as this factor is inversely correlated with temperature (Mushore et al., 2018; Zhang et al., 2018).

Satellite data processing

This study generated raster layers of LST and land cover classes using the Landsat 8 — Operational Land Imager (OLI) — images of 30 m spectral resolution. LST was calculated following an approach by He et al. (2019), who retrieved LST using spectral bands of Thermal InfraRed Sensor (TIRS) 10 in Landsat 8. The pixel-based estimates were distributed at ward scale. The land cover classification was carried

Table 1.
Summary of data used in this study.

Variables		Description	Unit	Data Source
Latent	Observed			
Exposure	Land Surface Temperature (LST)	Pixel wise (30 m resolution) LST	°C	United States Geological Survey (USGS), Landsat 8, May 2017
	Population Density	Number of people living in per km^2	p/km^2	(BBS, 2011)
Sensitivity	Elderly population	Number of old (>65 years) people per km^2	p/km^2	(BBS, 2011)
	Very young population	Number of children (<9 years) per km^2	"	"
	Illiteracy rate	The number of illiterate people per km^2 who cannot read or write a letter.	"	"
	Built-up area	All infrastructure- residential, commercial, mixed use and industrial areas, villages, settlements, road network, pavements, and man-made structures. The ratio of the total pixel of built-up area and the total pixel of the ward was considered.	Pixel ratio	USGS, Landsat 8, May, 2017
	Poverty	Number of people per km^2 living below poverty line.	p/km^2	(WB, 2011)
	Access to water	The number of people per km^2 having limited access to the water supply.	"	(BBS, 2011)
	Female population	Number of females living in per km^2	"	"
	Unemployment	The number of people per km^2 who were not involved in any work or were looking for work	"	"
	Occupation	The number of people per km^2 susceptible to heat related illnesses due to involvement in occupations such as industrial and agricultural work.	"	"
	Disability	The number of people per km^2 having a vision, auditory, speech impairment and physical, mental disability and autism.	"	"
Adaptive capacity	Access to electricity	Number of people per km^2 having electricity connection in their houses.	p/km^2	(BBS, 2011)
	Vegetation	Represents trees, natural vegetation, mixed forest, gardens, parks and playgrounds, grassland, vegetated lands, agricultural lands, and crop fields. The area occupied by a vegetative cover of any given ward divided by respective ward's total area was considered.	Pixel ratio	USGS, Landsat 8, May, 2017
	Road	Area occupied by the road of any given ward divided by the total area of the respective ward.	Area ratio	(CDA, 2009)
	Waterbody	Represents water features such as a river, permanent open water, lakes, ponds, canals, permanent/seasonal wetlands, low-lying areas, marshy land, and swamps. The area occupied by any given ward's water features divided by respective ward's total area was considered.	Pixel ratio	USGS, Landsat 8, May, 2017

out applying a widely used supervised classification technique with the maximum likelihood algorithm in GIS (Abdullah et al., 2019). This classification technique was used due to its robustness and potentiality of producing precise land cover classes (Sisodia et al., 2014). Land cover data generated for the study area included four classes: built-up area, vegetation, waterbody, and others (Table S1, supplementary document). Classification accuracy of land cover data was assessed by estimating the Kappa-coefficient (Landis and Koch, 1977). Therefore, 400 ground-truthing points were collected from the primary field survey. The overall accuracy of this classification was 80.75%, with an acceptable kappa-coefficient of 0.744.

Factor analysis and normalizing HVI

Selected indicators of HVI could be subject to multicollinearity. Therefore, Pearson's correlation coefficients were estimated to check the indicators' relationship (Schober et al., 2018). Most of the observed variables were correlated to each other. Therefore, factor analysis was performed to avoid multicollinearity and limit the complexity of data by reducing their dimensions (Basilevsky, 2009; Cutter et al., 2003; Harlan et al., 2013). For measuring the sampling adequacy and the usefulness of the results of factor analysis, Kaiser-Meyer-Olkin (KMO) and Bartlett's test of sphericity were carried out (Williams et al., 2010). The KMO values of exposures, sensitivity, and adaptive capacity were estimated to be 0.50, 0.807, and 0.667, respectively. The *p*-value of less than 0.05 indicated that the results were statistically significant. Then factor analyses on the standardized dataset (mean = 0 and variance = 1) of all latent variables were conducted individually. Orthogonal varimax rotation and Kaiser-eigenvalue criteria (eigenvalue>1) were used to extract independent components. The varimax rotation was used because of its ability to extract maximum independent components and to ensure maximum loading of variables into the components (Kim and Mueller, 1978). The Anderson–Rubin method was applied to measure factor scores as the Bartlett and Regression methods tend to extract correlated factors (Basilevsky, 2009; Harman, 1976). The estimated scores were included in Eq. (1) to calculate the HVI score. Then ward-wise HVI scores were normalized at a 0 to 1 scale using Eq. (2) (Inostroza et al., 2016).

$$\beta = \left[\frac{x - x_{min}}{x_{max} - x_{min}}\right] \quad (2)$$

where β is the normalized HVI value at each ward, x is the original HVI value, x_{min} and x_{max} are the lowest and highest HVI values, respectively.

Obtained normalized HVI values were categorized into five classes — very low, low, moderate, high, and very high — applying the Jenks optimization method in GIS (Aubrecht and Özceylan, 2013).

Deriving spatial distribution of HVI

This study carried out spatial statistical analyses to estimate the spatial distribution of HVI in the CCC area. Three different spatial statistical methods were applied: Spatial autocorrelation (Global Moran's I), Clus-

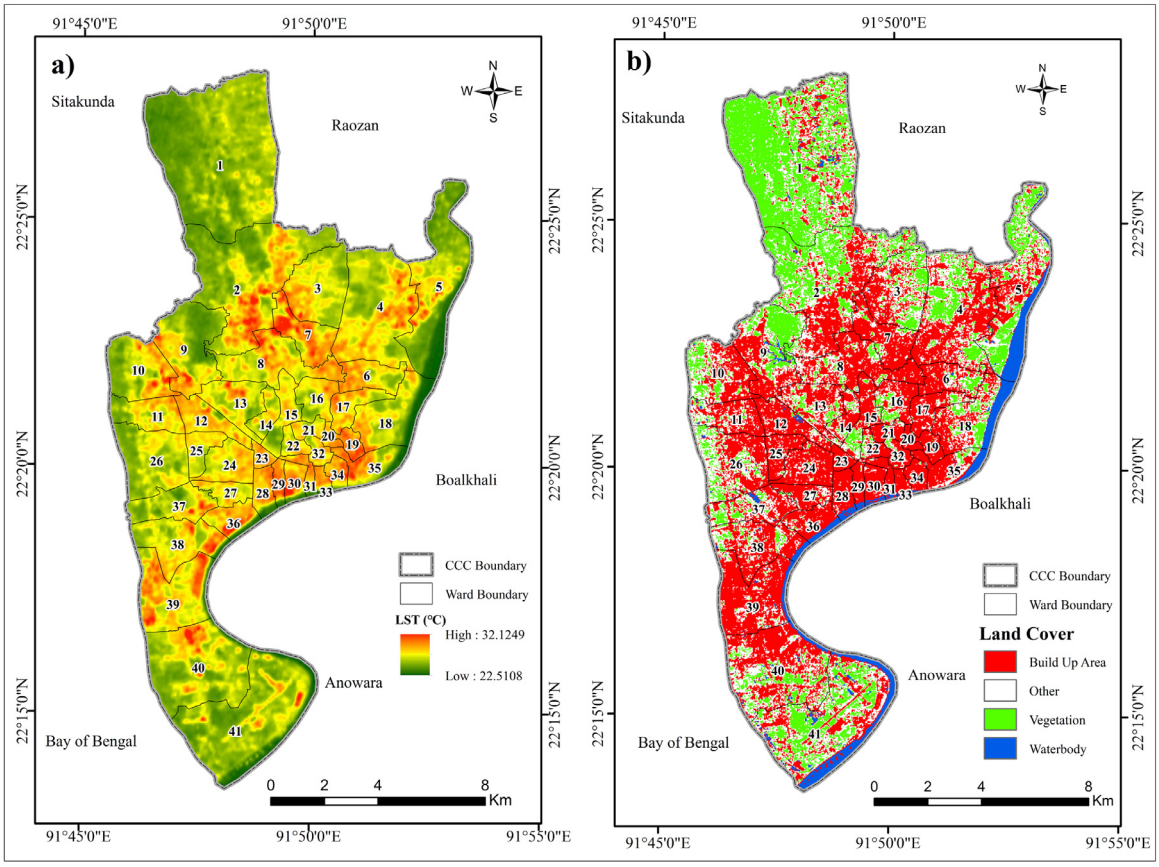

Fig. 2. (a) Pixel-based Land surface Temperature (LST) and (b) Land Cover map.

ter and Outlier Analysis (Anselin Local Moran's I), and Hot Spot Analysis (Getis-Ord Gi*).

Analyzing spatial autocorrelation

The spatial autocorrelation of HVI across the CCC area was tested by estimating Global Moran's I coefficients that indicate whether the pattern expressed was clustered, dispersed, or random (Getis and Ord, 2010; Goodchild, 1986). A negative Moran's I index value represents a tendency towards dispersion, while a positive value indicates a tendency towards clustering; zero indicates no autocorrelation (random). The *z*-score and *p*-value indicate the statistical significance of the coefficients. This method hypothesizes that data is randomly distributed. To reject the null hypothesis, the *p*-values should be less than 0.1 at a 90% confidence interval (10% significance level), whereas the *z*-scores should be less than (<) −1.65 and greater than (>) +1.65 (Getis and Ord, 2010).

Cluster and outlier analysis

This study carried out cluster and outlier analyses by estimating local Moran's I index to identify the spatial cluster of HVI in various wards of CCC (Anselin, 1995; Mitchel, 2005). In this method, an index value is estimated for each feature representing the neighboring features with similar (cluster) or dissimilar (outlier) high or low attribute values. The *z*-score and *p*-value determine the statistical significance of the estimated index value. A positive index indicates similarity for neighboring features, where a negative index represents dissimilarity. Four types of cluster/outlier were found as statistically significant such as cluster of high value (HH), cluster of Low value (LL), an outlier with high value surrounded by low primary value (HL), and outlier with low value primarily surrounded by high values (LH).

Hot spot analysis

In this study, a hot spot analysis was performed using Getis-Ord Gi* statistics (pronounced G-i-star) (Getis and Ord, 1992, 2010) to find statistically significant hot spots (clustering of high values)/cold spots (clustering of low values) of HVI in CCC areas. A statistically significant hot spot indicates a feature (ward) with a high value and/or is surrounded by other features (wards) with high values. Contrarily, a cold spot means a feature with a very low value and/or is surrounded by other features (wards) with low values. As high HV influences the adjacent area and the nature of heat hazard regulates the impact, contiguity edge was only utilized to conceptualize spatial relationship and was used during the computation of Gi* in GIS. It estimated Gi* of each feature in the dataset, which is a *z*-score. It also calculated the *p*-value of each feature in the dataset to identify the statistically significant features. A *z*-score greater than 1.65 and a *p*-value less than 0.1 is considered a statistically significant hotspot/cold spot at a 90% confident level (Sánchez-Martín et al., 2019). Conversely, a *z*-score less than −1.65 and a *p*-value less than 0.1 are considered the statistically significant cold spot at a 90% confidence level. A 90% confidence level was considered in this study to detect all the probable hotspots.

Results and discussion

Spatial distribution of lst in CCC

Fig. 2(a) shows the spatial distribution of LST distribution in CCC. The mean LST was found to be 25.30 °C with a standard deviation of 1.25. Several hotspots can be observed in Fig. 2(a), where the temperature ranges between 28.87 °C and 32.08 °C. It is not a surprise that the value of LST was higher in areas classified as built-up areas (~45% of

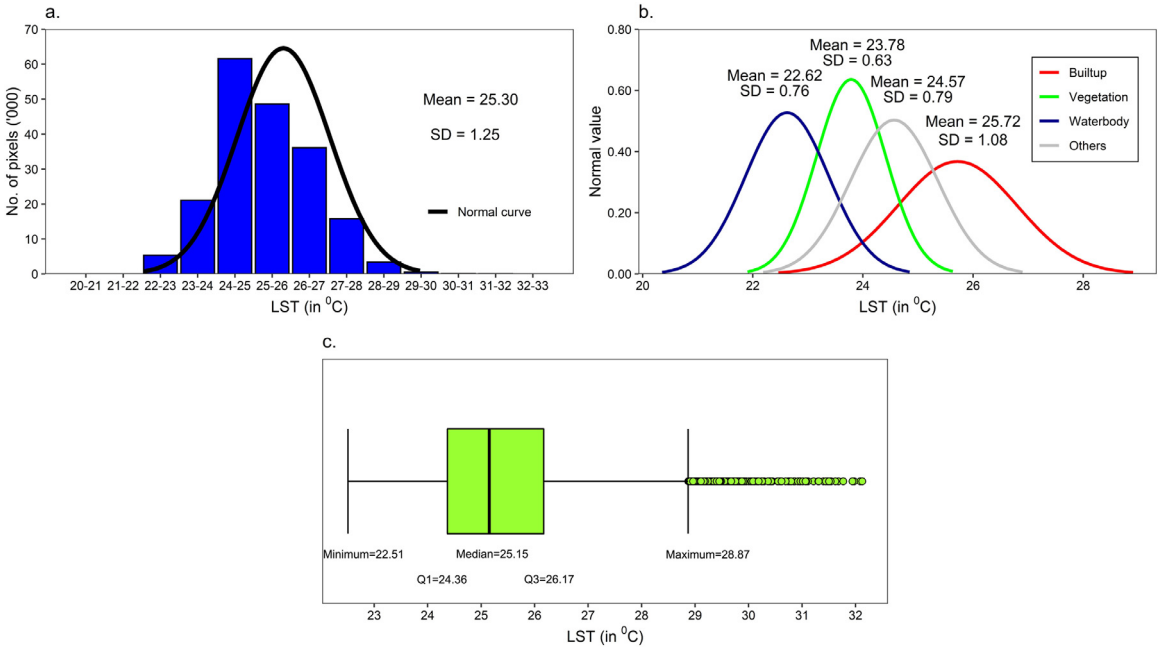

Fig. 3. (a) Normal distribution curve of observed LST (b) Normal distribution curve of observed LST according to different land cover classes (c) Box plot of LST distribution.

Table 2.
Result of component extraction of factor analysis.

Variables	Components	Standard deviation	Proportion of variance	Cumulative proportion	Factor Score	Description (factor score)
Exposure	1	1.70	85.14	85.14	−1.83 to 3.10	(-) low exposure (+) high exposure
Sensitivity	1	6.81	68.13	68.13	−1.47 to 3.12	(-) low sensitivity (+) high sensitivity
	2	1.16	11.64	79.77	−1.52 to 3.51	
Adaptive Capacity	1	2.26	56.38	56.38	−2.90 to 1.51	(-) low adaptive capacity (+) high adaptive capacity
	2	1.04	25.93	82.31	−1.10 to 1.96	

the total area) (Fig. 2(b)). A significant negative correlation exists (Pearson correlation coefficient −0.439) between LST and NDVI. The density of built-up area was the highest in the middle part of the city where the proportion of other land use types was small. Those areas are characterized by a higher degree of LST. LST was low in the northern part of the study area, which is mostly covered with vegetation. The average LST of built-up, vegetation, and water body were 25.72 ^{0}C, 23.78 ^{0}C, and 22.62 ^{0}C, respectively, with corresponding standard deviations of 1.08, 0.63, and 0.76 (Fig. 3).

Factor analysis

The component extraction results of factor analysis are summarized in Table 2. In the case of exposure, one component was extracted (score ranged from −1.83 to 3.10), based on Kaiser Eigenvalue criteria (eigenvalue>1), which explained about 85% variability of the input dataset.

For variables related to sensitivity, two components were extracted (Pohlmann, 2004) that cumulatively explained 79.773% variability of the data. Similarly, two components were found for variables related to the adaptive capacity that explain 82.31% variability of the input indicators. As multiple components were extracted, the orthogonal axis rotation (varimax) was used for higher loadings of variables. The rotation was completed in 3 iterations, and the variance explained by components 1 and 2 were 68.13% and 11.64%, respectively. After axis rotation, the first component yielded a very high eigenvalue (6.43), explaining about 64.27% variability of the dataset, while the variance of the second component increased to 15.50%. In component 1, most of the variables yielded high positive factor loadings (*L*) (Table 3). Demographic and socioeconomic characteristics of people are significantly associated with the sensitivity aspect of heatwave vulnerability. For instance, heatwave vulnerable groups include female (L: 0.98), children (L: 0.95), disable (L: 0.93), unemployed (L: 0.88), illiterate (L: 0.87), and older people (L: 0.87). Factor 2 presents strong positive loading on the variable poverty, indicating that areas where a substantial number of people live below the poverty line are more vulnerable to the heatwave. Similar evidence was found in the work of Asefi-Najafabady et al. (2018).

Two components were extracted from the four observed variables of adaptive capacity (Table 2), explaining around 82.306% of the input variables' variance. The first component accounted for explaining around 56.380% of the total variance, while the second factor explained 25.926% variability of the input dataset. The axis rotation was completed in three iterations where the first and second components could explain 55.362% and 26.944% of the total variance, respectively. Higher factor loadings were found for three variables: vegetation (L: −0.891), road (L: 0.863), and electricity (L: 0.820). Negative loading for vegetation indicates that areas with a higher share of vegetation cover are less vulnerable to the heatwave. However, places which are occupied by roads are more vulnerable to this hazard. Access to electricity is a measure of urbanization. Urbanized areas are highly prone to heatwave

Table 3.
Factors loading of the input variables.

Variables		Components	
Latent	Observed	1	2
Exposure	Population Density	0.923	N/A
	LST	0.923	N/A
Sensitivity	Females	0.980*	0.119
	Children	0.955*	0.256
	Disable	0.925*	0.224
	Unemployed	0.878*	0.365
	Illiterate	0.869*	0.421
	Old people	0.869*	−0.197
	Built-up area	0.802*	−0.052
	Occupation	0.744*	0.543
	Without water supply	0.471*	0.003
	Poor	−0.024	0.880*
Adaptive Capacity	Vegetation	−0.891*	−0.135
	Road	0.863*	−0.057
	Electricity	0.820*	−0.298
	Waterbody	−0.047	0.984*

* *Statistically significant*.

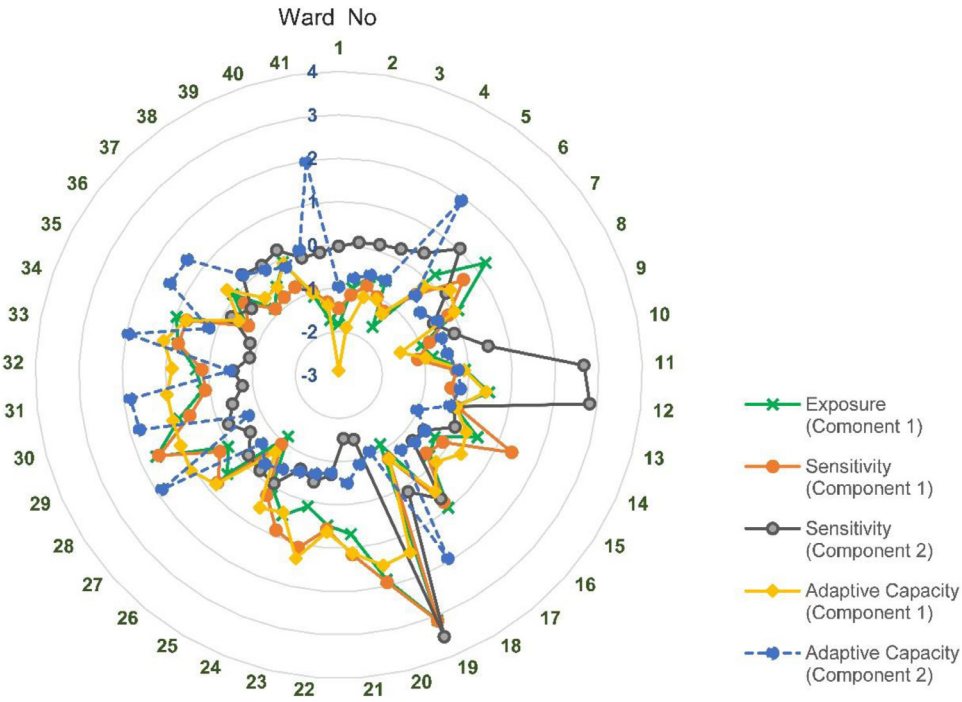

Fig. 4. Ward-wise variation in factor scores for different components of heat wave vulnerability.

vulnerability. Although an inverse relationship was observed between waterbody and LST, component 2 of this variable has a positive loading. Waterbodies comprised a very small proportion (5.32%) of the total study area that are mainly located in the eastern segment (Fig. 2(b)). Therefore, the influence of waterbodies in reducing heatwave vulnerability is low compared to parameters related to exposure and sensitivity.

The estimated factor scores for different components were disaggregated at ward scale (Fig. 4). In the case of exposure, factor scores in most of the wards were higher (score ranges between 0 and 2), with the highest score in ward no 19. A negative sensitivity score was estimated in most of the wards, while only three wards (ward no 11, 12, and 19) yielded high scores. In the case of adaptive capacity, component 02 had a higher variation in score than component 01. In component 1, most of the wards had a slight variation in scores distributed between −1 and +1. In the second component, estimated factor scores in most of the wards are negative, with only a few wards such as 5, 18, 28, 30, 31, 33, 35, 36, and 41 resulted in higher factor scores.

The HVI for CCC

Fig. 5(a, b, c) shows the spatial variation of exposure, sensitivity, and adaptive capacity, respectively. The mean of exposure was 0 with a standard deviation of 1. In the case of sensitivity and adaptive capacity, the mean was 0 with a standard deviation of 1.41. Therefore, the variation of the score of sensitivity and adaptive capacity was higher than exposure. In relation to exposure, the central CCC area (where ward no 7, 20, 19, and 29 are located) was highly exposed to heatwave than the peripheral area. In the case of sensitivity, the scores were relatively higher in wards 11, 12, 14, 17, 19, and 29. Although the northern end of the study area was relatively less ex-

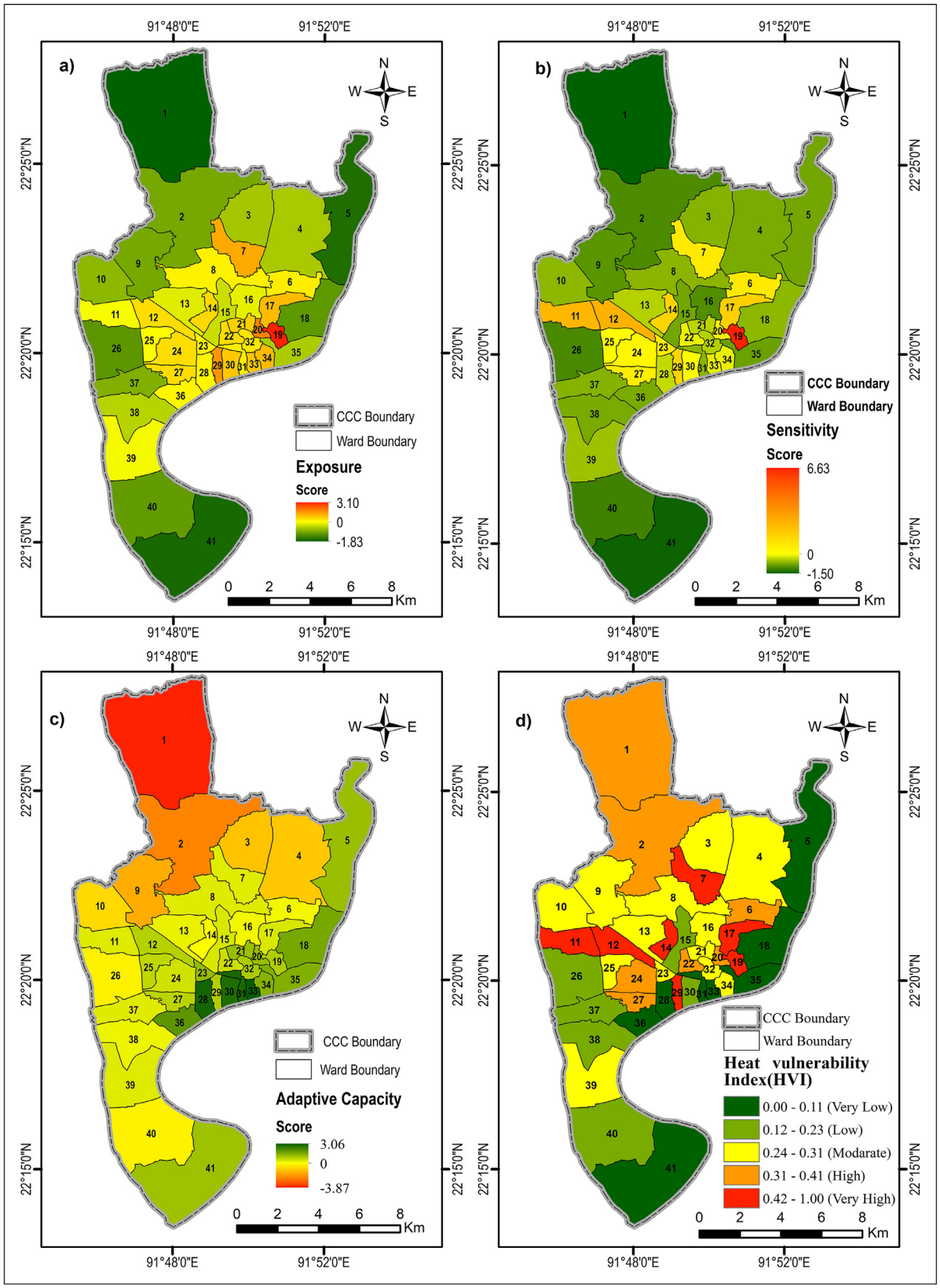

Fig. 5. Spatial variation of (a) exposure, (b) sensitivity, (c) adaptive capacity, and (d) heat vulnerability index in CCC.

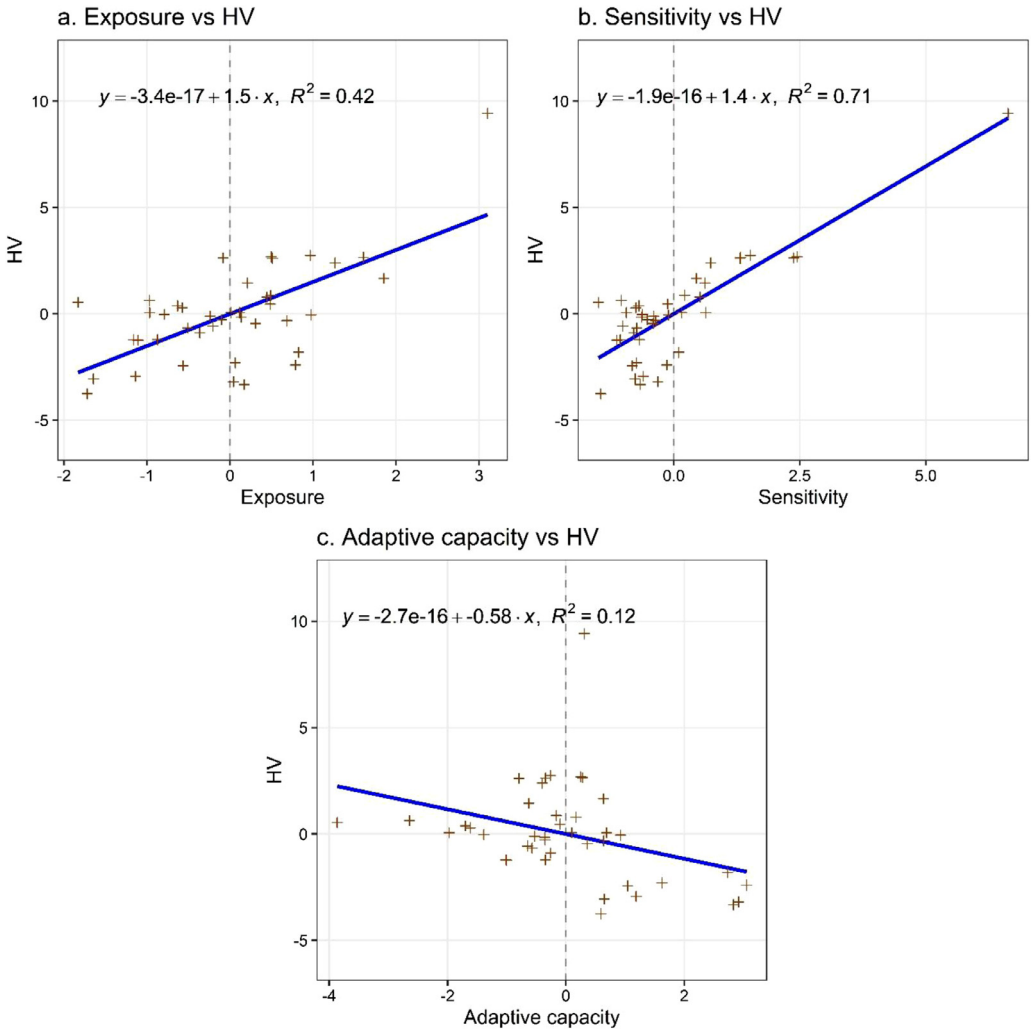

Fig. 6. Relationship of Exposure (*E*), Sensitivity(*S*) and Adaptive Capacity (*A*) with Heatwave vulnerability (HV).

posed to the heatwave, it was also characterized as less adaptive to this hazard.

Exposure and sensitivity are positively correlated with HVI with coefficients of determination (R^2) values 0.42 (p-value 0.001) and 0.71 (p-value 0.001), respectively, while adaptive capacity is negatively correlated (R^2 = 0.12, p-value 0.05) (Fig. 6). Similar evidence was found in a recent study (Inostroza et al., 2016). The resultant HVI for CCC is shown in Fig. 5(d). Notably, the correlation between adaptive capacity and HV is weak. This is because the adaptive capacity score in most of the wards is relatively low regardless of their exposure and sensitivity scores, which can be either low (e.g., ward 26, 37, 38) or high (e.g., wards 11, 12, 14) (Fig. 5). This study also noted that adaptive capacity of ward 1 is very low (Fig. 5(c)). The ward is in a hilly area where very few people live. While the area is covered by vegetation, values of other three indicators of adaptive capacity: the presence of electricity, water bodies, and road, were found to be very low. Among 41 wards, seven (7.61% of the total area) were found to be very highly vulnerable to heatwave, where the mean HVI is 0.56. These areas are characterized by high population density and built-up areas. 'Moderate' and 'high' degree of heatwave vulnerability classes comprised 28 0.54% and 26.40% of the total study area, respectively. The remaining 14 wards were classified as low and very low vulnerable areas to the heatwave, accounting for 37.45% of the total area (Table S2, supplementary document).

The degree of influence of different observed variables on HVI was also estimated by subtracting mean values of all variables between very high and very low vulnerable areas (Table S3, supplementary document). All observed variables related to exposure and sensitivity were found to be positively associated with HVI. However, only two variables (i.e., vegetation and waterbody) related to adaptive capacity were negatively associated with HVI.

Spatial distribution of HVI

Results of spatial autocorrelation (Global Moran's I), cluster and outlier (Anselin Local Moran's I), and hot spot (Getis-Ord Gi*) analyses indicate the pattern of the spatial distribution of HVI in the CCC area. The spatial autocorrelation value of 0.01, with a low z-score (0.4) and a high p-value (0.69), indicates that the spatial pattern of HVI was randomly distributed. Since Global Moran's I measured the spatial pattern of HVI for the entire city, the presence of a local cluster was not apparent. To address this issue, Cluster and Outlier analyses were carried out. In the case of Cluster analysis, three different clusters, such as high-high cluster (HH), high-low outlier (HL), and low-low cluster (LL), were found to be statistically significant. A cluster of high-high (HH) HVI for ward 17 means this ward, along with the adjacent wards, was highly heat vulnerable zones.

In contrast, ward 40 had a cluster of Low-low (LL) HVI, indicating that this ward and the surroundings were less vulnerable to the heatwave. Although the HVI value for ward 29 was very high, a high-low outlier (HL) value was derived. The result indicates that ward 29 was

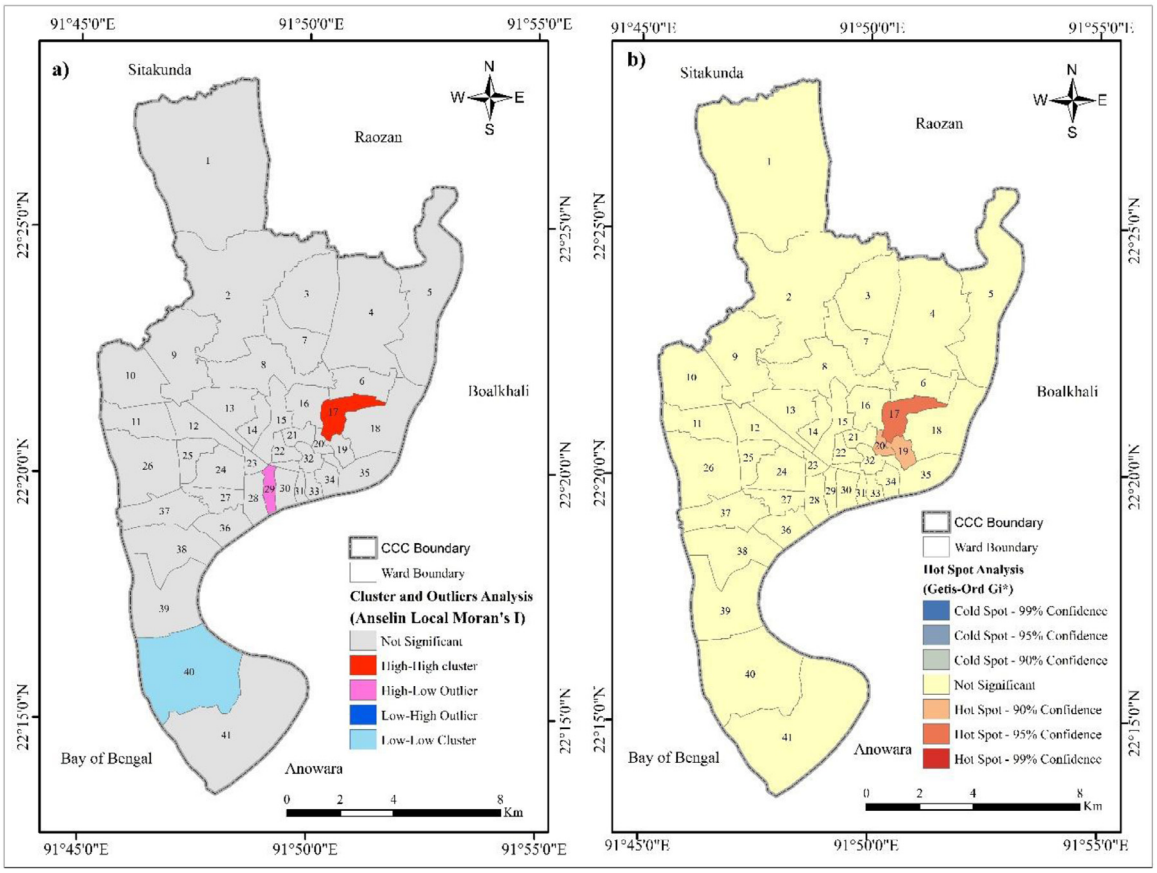

Fig. 7. (a) Cluster and Outlier Analysis for HVI and b) Hot Spot Analysis of HVI.

surrounded by areas with low HVI values. Fig. 7(a) shows the result of cluster and outlier analysis. Getis-Ord Gi* statistic was also applied to find either high or low heat vulnerable areas in CCC. The result shows that only three wards (ward no. 17, 19, and 20) were statistically significant hot spots (highly vulnerable) for HVI. The analysis, however, did not find any area of statistically significant cold spot (low vulnerable) for HVI (Fig. 7(b)).

Although the values of the Global Moran's I indicate that the spatial pattern of HVI was randomly distributed in CCC, higher LST was found in built-up areas. Many recent studies identified a positive correlation between LST with built-up areas (Ezimand et al., 2018; Inostroza et al., 2016; Raja, 2012; Roy et al., 2020; Zhang et al., 2017). Whilst exposure (i.e., LST) is similar in built-up areas, differences in sensitivity and adaptive capacity resulted in a heterogeneous distribution of HVI throughout CCC. This study found seven wards (ward no. 7, 11, 12,14,17, 19, and 29) with very highly vulnerable to the heatwave, and they are randomly distributed in the city. In the case of Anselin Local Moran's I, different statistically significant local clusters were found. As the heat transfer from a hot to a cold environment, the heat vulnerability may impact the High-High cluster (HH) and High-low outlier. Since ward 17 was surrounded by high HVI value areas, so this ward needed more time to cool down. Contrarily, ward 29 was surrounded by less vulnerable wards and, thus, less cooling time. From the hotspot analysis, contiguity of three wards — ward 17, 19, 20 — were found as statistically significant hot spot areas. Such a situation prevailed because the mean HVI of these three wards was much higher than the study area's global mean. Thus, they had a higher *z*-score (higher than +1.65) with a *p*-value of 0.1 and 0.05. From the cluster and hot spot analyses, it is evident that ward 17 and its surrounding areas, especially ward 19 and 20 were most vulnerable to heatwave hazard.

Conclusion

In recent years, the heatwave has become a significant problem in many urban areas. Rapid urbanization, high population growth, climate change, and transformation of land cover (from vegetation and water bodies to built-up areas) are causing an increase in the magnitude of this hazard. Consequently, heat-related diseases have increased in number, and a heat-sensitive group of inhabitants became more vulnerable in urban areas. Considering various complexities in understanding the impact of a heatwave, this study estimated heatwave vulnerability (HV) in the Chattogram City Corporation (CCC) area of Bangladesh based on three latent vulnerability parameters: exposure, sensitivity, and adaptive capacity. The results indicate that HV is strongly associated with sensitivity parameters. About 7.61% of CCC's total area was classified as being a very highly heatwave vulnerable area, while high and moderate classes included 26.40% and 28.54% area, respectively. A total of seven (out of 41) wards of CCC were identified as very high HV wards, which are seemingly scattered in the central part of the city. Generally, HVI was found to be randomly distributed in the city.

While this study contributes to quantifying HV using location-dependent climatic, socio-economic, physiological, and environmental parameters, it has several limitations. Due to the absence of observed temperature, this study relied upon the satellite-derived temperature. The Landsat images used in this study were acquired in the early morning (10:18 AM). However, air temperature becomes high during the noon and evening. Despite these limitations, this study presents a com-

prehensive framework for estimate HV. The methodology provided and the results obtained in this study will be of interest to planners and policymakers in identifying factors associated with HV. The framework provided in this study would enable them to prepare mitigation plans, policies, and strategies and sequencing and prioritizing adaption measures according to the degree of HV.

Declaration of Competing Interest

The authors declare that they have no known competing financial interests or personal relationships that could have appeared to influence the work reported in this paper.

Acknowledgment

This work is funded by Directorate of Research and Extension (DRE) of Chittagong University of Engineering and Technology (CUET) (Grant number - CUET/DRE/2017-2018/URP/002). The authors are pleased to express their gratitude to the Department of Urban and Regional Planning of CUET for providing logistic support to carry out this study.

Supplementary materials

Supplementary material associated with this article can be found, in the online version, at doi:10.1016/j.envc.2021.100122.

References

Abdullah, A.Y.M., Masrur, A., Adnan, M.S.G., Baky, M., Al, A., Hassan, Q.K., Dewan, A., 2019. Spatio-temporal patterns of land use/land cover change in the heterogeneous coastal region of Bangladesh between 1990 and 2017. Remote Sens. 11, 790.

Adnan, M.S.G., Dewan, A., Zannat, K.E., Abdullah, A.Y.M., 2019. The use of watershed geomorphic data in flash flood susceptibility zoning: a case study of the Karnaphuli and Sangu river basins of Bangladesh. Nat. Hazards 99, 425–448.

Ahmed, B., Kamruzzaman, M., Zhu, X., Rahman, M., Choi, K., 2013. Simulating land cover changes and their impacts on land surface temperature in Dhaka, Bangladesh. Remote Sens. 5, 5969–5998.

Aldrich, N., Benson, W.F., 2008. Disaster preparedness and the chronic disease nedds of vulnerable older adults. Prev. Chronic Dis. 1–7.

Anselin, L., 1995. Local indicators of spatial association—LISA. Geogr. Anal. 27, 93–115.

Ara, S., Islam, M.A., Showkat, S., 2016. Effect of land-use intensity on surface temperature: a study on Chittagong city corporation area. In: Proceedings of the 5th International Conference on Informatics, Electronics and Vision (ICIEV). IEEE, pp. 72–77.

Arrighi, J., Burkart, K., Nissan, H., 2017. Raising awareness on heat related mortality in Bangladesh. American Geophysical Union, Fall Meeting 2017, Bibcode: 2017AGUFMPA12A..06A.

Asefi-Najafabady, S., Vandecar, K.L., Seimon, A., Lawrence, P., Lawrence, D., 2018. Climate change, population, and poverty: vulnerability and exposure to heat stress in countries bordering the Great Lakes of Africa. Clim. Change 148, 561–573.

Aubrecht, C., Özceylan, D., 2013. Identification of heat risk patterns in the US national capital region by integrating heat stress and related vulnerability. Environ. Int. 56, 65–77.

Azhar, G., Saha, S., Ganguly, P., Mavalankar, D., Madrigano, J., 2017. Heat wave vulnerability mapping for India. Int. J. Environ. Res. Public Health 14, 357.

Basagaña, X., Sartini, C., Barrera-Gómez, J., Dadvand, P., Cunillera, J., Ostro, B., Sunyer, J., Medina-Ramón, M., 2011. Heat waves and cause-specific mortality at all ages. Epidemiology 765–772.

Basilevsky, A.T., 2009. Statistical Factor Analysis and Related methods: Theory and Applications. John Wiley & Sons.

BBS, 2011. District statistics 2011 - Chittagong in: Statistics, B.B.o. (Ed.), Dhaka, Bangladesh.

BMD, 2019. Annual Rainfall and Temperature Analysis. Bangladesh Metrological Department (BMD).

Borsboom, D., Mellenbergh, G.J., Van Heerden, J., 2003. The theoretical status of latent variables. Psychol. Rev. 110, 203.

Burkart, K., Breitner, S., Schneider, A., Khan, M.M.H., Krämer, A., Endlicher, W., 2014. An analysis of heat effects in different subpopulations of Bangladesh. Int. J. Biometeorol. 58 (2), 227–237.

Buscail, C., Upegui, E., Viel, J.F., 2012. Mapping heatwave health risk at the community level for public health action. Int. J. Health Geogr. 11, 1–9.

CDA, 2009. Preparation of Detailed Area Plan (DAP) For Chittagong Metropolitan Master Plan (CMMP). Chittagong Development Authority, Chittagong.

Chen, K., Horton, R.M., Bader, D.A., Lesk, C., Jiang, L., Jones, B., Zhou, L., Chen, X., Bi, J., Kinney, P.L., 2017. Impact of climate change on heat-related mortality in Jiangsu Province, China. Environ. Pollut. 224, 317–325.

Christenson, M., Geiger, S.D., Phillips, J., Anderson, B., Losurdo, G., Anderson, H.A., 2017. Heat vulnerability index mapping for Milwaukee and Wisconsin. J. Public Health Manag Pract. 23, 396–403.

Cutter, S.L., Boruff, B.J., Shirley, W.L., 2003. Social vulnerability to environmental hazards. Soc. Sci. Q. 84, 242–261.

Dewan, A., Kiselev, G., Botje, D., Mahmud, G.I., Bhuian, M.H., Hassan, Q.K., 2021. Surface urban heat island intensity in five major cities of Bangladesh: patterns, drivers and trends. Sustain. Cities. Soc., 102926.

Dewan, A.M., Corner, R.J., 2012. The impact of land use and land cover changes on land surface temperature in a rapidly urbanizing megacity. In: Proceedings of the IEEE International Geoscience and Remote Sensing Symposium, pp. 6337–6339.

Dewan, A.M., Yamaguchi, Y., 2009. Land use and land cover change in Greater Dhaka, Bangladesh: using remote sensing to promote sustainable urbanization. Appl. Geogr. 29, 390–401.

Dole, R., Hoerling, M., Perlwitz, J., Eischeid, J., Pegion, P., Zhang, T., Quan, X.W., Xu, T., Murray, D., 2011. Was there a basis for anticipating the 2010 Russian heat wave? Geophys. Res. Lett. 38.

Ezimand, K., Kakroodi, A., Kiavarz, M., 2018. The development of spectral indices for detecting built-up land areas and their relationship with land-surface temperature. Int. J. Remote Sens. 39, 8428–8449.

Field, C.B., Barros, V., Stocker, T.F., Dahe, Q., 2012. Managing the Risks of Extreme Events and Disasters to Advance Climate Change adaptation: Special Report of the Intergovernmental Panel On Climate Change. Cambridge University Press.

Gazi, M.Y., Rahman, M.Z., Uddin, M.M., Rahman, F.A., 2020. Spatio-temporal dynamic land cover changes and their impacts on the urban thermal environment in the Chittagong metropolitan area, Bangladesh. GeoJournal 1–16.

Getis, A., Ord, J.K., 1992. The analysis of spatial association by use of distance statistics. Geogr. Anal. 24, 189–206.

Getis, A., Ord, J.K., 2010. The Analysis of Spatial Association By Use of Distance statistics. Perspectives on Spatial Data Analysis. Springer, pp. 127–145.

Goodchild, M.F., 1986. Spatial Autocorrelation. Geo Books.

Haines, A., Kovats, R.S., Campbell-Lendrum, D., Corvalán, C., 2006. Climate change and human health: impacts, vulnerability and public health. Public Health 120, 585–596.

Hajat, S., Kovats, R.S., Lachowycz, K., 2007. Heat-related and cold-related deaths in England and Wales: who is at risk? Occup. Environ. Med. 64, 93–100.

Harlan, S.L., Brazel, A.J., Prashad, L., Stefanov, W.L., Larsen, L., 2006. Neighborhood microclimates and vulnerability to heat stress. Soc. Sci. Med. 63, 2847–2863.

Harlan, S.L., Declet-Barreto, J.H., Stefanov, W.L., Petitti, D.B., 2013. Neighborhood effects on heat deaths: social and environmental predictors of vulnerability in Maricopa County, Arizona. Environ. Health Perspect. 121, 197–204.

Harman, H.H., 1976. Modern Factor Analysis. University of Chicago press.

Hassan, M.M., Nazem, M.N.I., 2016. Examination of land use/land cover changes, urban growth dynamics, and environmental sustainability in Chittagong city, Bangladesh. Environ. Dev. Sustain. 18, 697–716.

He, B.J., Zhao, Z.Q., Shen, L.D., Wang, H.B., Li, L.G., 2019. An approach to examining performances of cool/hot sources in mitigating/enhancing land surface temperature under different temperature backgrounds based on landsat 8 image. Sustain. Cities Soc. 44, 416–427.

Ho, H.C., Knudby, A., Huang, W., 2015. A spatial framework to map heat health risks at multiple scales. Int. J. Environ. Res. Public Health 12, 16110–16123.

Hoque, A., Clarke, A., 2013. Greening of industries in Bangladesh: pollution prevention practices. J. Clean. Prod. 51, 47–56.

Inostroza, L., Palme, M., de la Barrera, F., 2016. A heat vulnerability index: spatial patterns of exposure, sensitivity and adaptive capacity for Santiago de Chile. PLoS ONE 11, e0162464.

Johnson, D.P., Stanforth, A., Lulla, V., Luber, G., 2012. Developing an applied extreme heat vulnerability index utilizing socioeconomic and environmental data. Appl. Geogr. 35, 23–31.

Kim, D.W., Deo, R.C., Lee, J.S., Yeom, J.M., 2017. Mapping heatwave vulnerability in Korea. Nat. Hazards 89, 35–55.

Kim, J.-O., Mueller, C.W., 1978. Factor Analysis: Statistical methods and Practical Issues. SAGE.

Kinney, P.L., O'Neill, M.S., Bell, M.L., Schwartz, J., 2008. Approaches for estimating effects of climate change on heat-related deaths: challenges and opportunities. Environ. Sci. Policy 11, 87–96.

Kovats, R.S., Hajat, S., 2008. Heat stress and public health: a critical review. Annu. Rev. Public Health 29, 41–55.

Landis, J.R., Koch, G.G., 1977. The measurement of observer agreement for categorical data. Biometrics 159–174.

Lavell, A., 1999. Natural and Technological disasters: Capacity building and Human Resource Development For Disaster management. Concept Paper Commissioned By Emergency Response Division. United Nations Development Program, Geneva, Switzerland.

Liu, X., Yue, W., Yang, X., Hu, K., Zhang, W., Huang, M., 2020. Mapping urban heat vulnerability of extreme heat in hangzhou via comparing two approaches. Complexity 2020.

Mac, V.V.T., McCauley, L.A., 2017. Farmworker vulnerability to heat hazards: a conceptual framework. J. Nurs. Scholarsh. 49, 617–624.

Macnee, R.G., Tokai, A., 2016. Heat wave vulnerability and exposure mapping for Osaka City, Japan. Environ. Syst. Decis. 36, 368–376.

McGeehin, M.A., Mirabelli, M., 2001. The potential impacts of climate variability and change on temperature-related morbidity and mortality in the United States. Environ. Health Perspect. 109, 185–189.

McMichael, A.J., Wilkinson, P., Kovats, R.S., Pattenden, S., Hajat, S., Armstrong, B., Vajanapoom, N., Niciu, E.M., Mahomed, H., Kingkeow, C., 2008. International study of temperature, heat and urban mortality: the 'ISOTHURM'project. Int. J. Epidemiol. 37, 1121–1131.

Medina-Ramón, M., Zanobetti, A., Cavanagh, D.P., Schwartz, J., 2006. Extreme temperatures and mortality: assessing effect modification by personal characteristics and

specific cause of death in a multi-city case-only analysis. Environ. Health Perspect. 114, 1331–1336.
Méndez-Lázaro, P., Muller-Karger, F.E., Otis, D., McCarthy, M.J., Rodríguez, E., 2018. A heat vulnerability index to improve urban public health management in San Juan, Puerto Rico. Int. J. Biometeorol 62, 709–722.
Mitchel, A., 2005. The ESRI Guide to GIS analysis, Volume 2: Spartial measurements and Statistics. ESRI press.
Mushore, T.D., Mutanga, O., Odindi, J., Dube, T., 2018. Determining extreme heat vulnerability of Harare Metropolitan City using multispectral remote sensing and socio-economic data. J. Spat. Sci. 63, 173–191.
Nakai, S., Itoh, T., Morimoto, T., 1999. Deaths from heat-stroke in Japan: 1968–1994. Int. J. Biometeorol. 43, 124–127.
Nayak, S., Shrestha, S., Kinney, P., Ross, Z., Sheridan, S., Pantea, C., Hsu, W., Muscatiello, N., Hwang, S., 2018. Development of a heat vulnerability index for New York State. Public Health 161, 127–137.
Nissan, H., Burkart, K., Coughlan de Perez, E., Van Aalst, M., Mason, S., 2017. Defining and predicting heat waves in Bangladesh. J. Appl. Meteorol. Clim. 56, 2653–2670.
O'Neill, M.S., Zanobetti, A., Schwartz, J., 2003. Modifiers of the temperature and mortality association in seven US cities. Am. J. Epidemiol. 157, 1074–1082.
Ogbomo, A.S., Gronlund, C.J., O'Neill, M.S., Konen, T., Cameron, L., Wahl, R., 2017. Vulnerability to extreme-heat-associated hospitalization in three counties in Michigan. 2000–2009. Int. J. Biometeorol. 61, 833–843.
Patz, J.A., Campbell-Lendrum, D., Holloway, T., Foley, J.A., 2005. Impact of regional climate change on human health. Nature 438, 310–317.
Pohlmann, J.T., 2004. Use and interpretation of factor analysis in The Journal of Educational Research: 1992-2002. J. Educ. Res. 98 (1), 14–23.
Poumadere, M., Mays, C., Le Mer, S., Blong, R., 2005. The 2003 heat wave in France: dangerous climate change here and now. Risk Anal. Int. J. 25, 1483–1494.
Raja, D.R., 2012. Spatial analysis of land surface temperature in Dhaka metropolitan area. J Bangladesh Inst. Plan. ISSN 2075, 9363.
Reid, C.E., O'neill, M.S., Gronlund, C.J., Brines, S.J., Brown, D.G., Diez-Roux, A.V., Schwartz, J., 2009. Mapping community determinants of heat vulnerability. Environ. Health Perspect. 117, 1730–1736.
Rinner, C., Patychuk, D., Bassil, K., Nasr, S., Gower, S., Campbell, M., 2010. The role of maps in neighborhood-level heat vulnerability assessment for the city of Toronto. Cartogr. Geogr. Inf. Sci. 37, 31–44.
Roy, S., Pandit, S., Eva, E.A., Bagmar, M.S.H., Papia, M., Banik, L., Dube, T., Rahman, F., Razi, M.A., 2020. Examining the nexus between land surface temperature and urban growth in Chattogram metropolitan area of Bangladesh using long term Landsat series data. Urban Clim. 32, 100593.
Sánchez-Martín, J.M., Rengifo-Gallego, J.I., Blas-Morato, R., 2019. Hot spot analysis versus cluster and outlier analysis: an enquiry into the grouping of rural accommodation in Extremadura (Spain). ISPRS Int. J. Geo-Inf. 8, 176.
Schober, P., Boer, C., Schwarte, L.A., 2018. Correlation coefficients: appropriate use and interpretation. Anesth. Analg. 126, 1763–1768.
Semenza, J.C., Rubin, C.H., Falter, K.H., Selanikio, J.D., Flanders, W.D., Howe, H.L., Wilhelm, J.L., 1996. Heat-related deaths during the July 1995 heat wave in Chicago. N. Engl. J. Med. 335, 84–90.
Sisodia, P.S., Tiwari, V., Kumar, A., 2014. Analysis of supervised maximum likelihood classification for remote sensing image. In: Proceedings of the International Conference on Recent Advances and Innovations in Engineering (ICRAIE-2014). IEEE, pp. 1–4.
Tomlinson, C.J., Chapman, L., Thornes, J.E., Baker, C.J., 2011. Including the urban heat island in spatial heat health risk assessment strategies: a case study for Birmingham, UK. Int. J. Health Geogr. 10, 1–14.
Uejio, C.K., Wilhelmi, O.V., Golden, J.S., Mills, D.M., Gulino, S.P., Samenow, J.P., 2011. Intra-urban societal vulnerability to extreme heat: the role of heat exposure and the built environment, socioeconomics, and neighborhood stability. Health Place 17, 498–507.
WB, 2011. Poverty Maps of Bangladesh - 2010 Technical Report. World Bank (WB).
Wilhelmi, O.V., Hayden, M.H., 2010. Connecting people and place: a new framework for reducing urban vulnerability to extreme heat. Environ. Res. Lett. 5, 014021.
Williams, B., Onsman, A., Brown, T., 2010. Exploratory Factor analysis: A five-Step Guide For Novices. Australasian journal of paramedicine 8.
Wolf, T., McGregor, G., 2013. The development of a heat wave vulnerability index for London, United Kingdom. Weather Clim. Extre. 1, 59–68.
Zhang, W., McManus, P., Duncan, E., 2018. A raster-based subdividing indicator to map urban heat vulnerability: a case study in sydney, australia. Int. J. Environ. Res. Public Health 15, 2516.
Zhang, Y., Nitschke, M., Krackowizer, A., Dear, K., Pisaniello, D., Weinstein, P., Tucker, G., Shakib, S., Bi, P., 2017. Risk factors for deaths during the 2009 heat wave in Adelaide, Australia: a matched case-control study. Int. J. Biometeorol. 61, 35–47.
Zuhra, S.S., Tabinda, A.B., Yasar, A., 2019. Appraisal of the heat vulnerability index in Punjab: a case study of spatial pattern for exposure, sensitivity, and adaptive capacity in megacity Lahore, Pakistan. Int. J. Biometeorol. 63, 1669–1682.